

07,11,12,13

Heterogeneous nature of multistage solid-solid phase transitions in even normal alkanes — triacontane, dotriacontane and hexatriacontane

© A.K. Borisov, S.A. Gureva, V.M. Egorov, V.A. Marikhin

Ioffe Institute,
St. Petersburg, Russia

E-mail: Borisov.ak@mail.ioffe.ru

Received September 16, 2024

Revised September 16, 2024

Accepted September 17, 2024

A precision study of the phase transformation process during heating of n-alkanes: triacontane $C_{30}H_{62}$, dotriacontane $C_{32}H_{66}$ and hexatriacontane $C_{36}H_{74}$ was carried out using the differential scanning calorimetry method. Phase transformations in the solid state were considered from the point of view of the theory of diffuse phase transitions, which made it possible to distinguish three individual stages in the processes of transition development based on the analysis of the shape of heat capacity peaks and to conduct their independent analysis. A single mechanism of structural transformations from the initial monoclinic modification to the rotator phase through intermediate orthorhombic and monoclinic phases was established for the considered n-alkanes homologues. Each of the phase transformations was characterized in the approximation of heterogeneous development of the phase transition. The critical length of the n-alkane chain required for the implementation of the solid-solid phase transition was established.

Keywords: long-chain molecular crystal, n-alkane, phase transition, rotator-crystalline phase, differential scanning calorimetry.

DOI: 10.61011/PSS.2024.10.59636.238

1. Introduction

The temperature polymorphism of long-chain n-alkanes has been attracting the attention of researchers around the world for many years [1–8] because of the lack of consensus about the mechanism of structural rearrangements in case of the transition from a solid state to a melt and back. The main attention was paid to the study of structural transitions in n-alkanes C_nH_{2n+2} with the number of carbon atoms in the chain $n < 27$, since it was possible to identify with a sufficient reliability the presence of a number of intermediate phases occurring in them in heating/cooling processes [5,9–14]. Such intermediate phases between an isotropic liquid and a fully ordered crystalline state are called rotator phase (R) [15], which are characterized by the presence of discrete rotation of molecules around their main axes in the crystal cores of lamellae with a certain number of equally probable orientations for each of rotator phases. It is important to note that n-alkanes form a supermolecular structure of plates during crystallization from the melt which are called lamellae. Individual lamellas are stacked in tightly packed stacks inside which a crystalline core composed of three-dimensionally packed methylene sequences and the lamella surface formed by terminal methyl groups are defined. Two types of crystal cells are considered in n-alkane crystals [16]: the main cell, which characterizes the way lamellae are stacked relative to each other in stacks, and the subcell, which describes the nature of the stacking

of methylene trans-sequences in the crystalline cores of individual lamellae.

Currently, five different rotator phases R are considered for n-alkanes, depending on the chain lengths and the initial symmetry of the crystals [2,3]. The rotator phases differ from each other in the types of crystalline main cells and subcells, as well as in the number of equally probable orientations of molecules in subcells associated with the rotations of molecules around their main axes. Three of them are well characterized: R_I , R_{II} and R_V , characteristic specifically for n-alkanes with $n < 27$ carbon atoms [5,9–12]. However, the homologues of n-alkanes with high values n are characterized by rotator phases R_{III} and R_{IV} , the little-studied features of which are of considerable interest for research. It was found in Ref. [13] that phase R_{III} is characterized by a triclinic main lattice cell, and phase R_{IV} is characterized by monoclinic main lattice cell, while the subcells are pseudo-hexagonal in both cases. In addition, it is shown that both structures are single-layered, but close to double-layered, which is determined by the period of repeatability in lamellar stacks. In both cases, the molecules are inclined relative to the axis perpendicular to the plane of the lamella at angles from 0 to 15° . The exact parameters of both the main cells and subcells of the phases R_{III} and R_{IV} are not determined presently.

The nature of the factors influencing the processes of temperature restructuring of n-alkanes has not yet been clarified. It has now been established that molecules not

only perform rotatory movements around their long axes (probably associated with longitudinal translations [17]), but they also undergo conformational changes in R phases that disrupt the molecular symmetry of a certain crystalline phase [18,19]. Since the proportion of molecules with conformational defects increases with the increase of the length of chain n , we assume that the number of defective molecules above a certain limit concentration induces the occurrence of a different molecular symmetry, which results in the formation of new rotatory crystal structures. For example, it can be assumed that the disappearance of the plane of specular reflection perpendicular to the long axis of the molecule in n -alkanes with an even number of carbon atoms n causes the formation of structures with molecules inclined relative to the base planes of the lamellae. However, a similar explanation of the difference in the features of R phases for n -alkanes with n below and above $n = 27$ is currently unproven.

It can be concluded from the above that there is a need for additional study to clarify the features of the phase behavior of long-chain n -alkanes. This paper is devoted to the study of phase transformations in the homological series of even n -alkanes: $C_{30}H_{62}$, $C_{32}H_{66}$, $C_{36}H_{74}$.

n -alkanes with an even number of carbon atoms in the chain $28 \leq n \leq 36$ have a monoclinic structure (main cell) defined for hexatriacontane $C_{36}H_{74}$ [20] with crystallographic space group $P2_1/a$ and point group C_{2h}^5 . At the same time, the stacking of molecules in lamellae, i.e. the subcell, is characterized by orthorhombic symmetry (space group P_{bnm} and point group D_{2h}^{16}).

The greatest attention was paid to hexatriacontane $C_{36}H_{74}$ among the above sequence of even homologues in the literature. For instance, possible structures of the main hexatriacontane cells are defined as monoclinic and orthorhombic in the Ref. [20–22]. In addition, the author of Ref. [4,23–27] noted that n - $C_{36}H_{74}$ crystals demonstrate a solid-solid phase transition from a monoclinic structure to a rotator phase R_{III} in the temperature range of ~ 70 – 75°C . However, the equally interesting behavior of the structure of $C_{36}H_{74}$ is also manifested at lower temperatures [28]. Hexatriacontane exhibits a low-temperature monoclinic (M_{011}) modification at room temperature in which the molecules are inclined in the plane bc relative to the lamellar surface. The crystal already demonstrates a high-temperature monoclinic (M_{101}) modification as the temperature increases, in which the molecules are tilted in ac -planes, this state persists until the transition to the rotator phase. The authors of Ref. [26] suggested that an intermediate vertical structure should occur during the transition from M_{011} to M_{101} . Later, this theory was supported by the authors of Ref. [29,30], indicating the occurrence of orthorhombic (O) modification. They suggested that the molecules move from an inclined arrangement in the bc -planes to a vertical structure, forming some intermediate activated state, and then tilt again, but already in the ac -planes. Subsequently, the authors of Ref. [31] experimentally confirmed the occurrence of an intermediate orthorhombic O phase.

It should be emphasized that the phase transition between two monoclinic phases in case of heating of hexatriacontane ($T = 72.0$ – 73.5°C) turns out to be irreversible, and the n -alkane remains in a high-temperature modification M_{101} in case of subsequent cooling [26,29,30]. It is believed that this is attributable to the fact that a change of the direction of inclination of the molecules in the lamellae to $+90^\circ$ or -90° has an equal probability. Thus, the M_{101} phase is a polycrystal, which is accompanied by the occurrence of numerous defects that make it difficult to reverse the transformation during the cooling process [29].

Similar studies were conducted for dotriacontane $C_{32}H_{66}$ [26] due to the similarity of homologue structures. However, the modification M_{101} was not found in case of the transition from M_{011} to the rotator R_{III} (the existence of the latter was established by many authors [2,4,13,31]). It was suggested that an intermediate modification M_{101} should also occur in the dotriacontane due to the identical initial and final phases in these homologues despite the fact that the corresponding peak of heat capacity could not be resolved. It is likely that this particular transition was recorded by the authors of Ref. [32] using the method of super-sensitive differential scanning calorimetry (DSC). They found an additional weak peak ($T = 65^\circ\text{C}$) on the dotriacontane thermogram in case of heating, preceding the rotatory transition ($T = 66^\circ\text{C}$). Moreover, it was possible to identify the transition R_{IV} – R_{III} during cooling at 68°C , due to the presence of temperature hysteresis, which was not observed during heating.

Triacontane $C_{30}H_{62}$ is considered in less detail in the literature [2–4,13]. Currently, no additional monoclinic modifications are identified for this homologue, except for the low-temperature M_{011} , but at the same time two rotator phases R_{III} and R_{IV} are identified with transition temperatures $T = 61^\circ\text{C}$ and $T = 63^\circ\text{C}$, respectively.

It can be concluded that monoclinic M_{011} is the initial structure in the homologues mentioned above, and the occurrence of rotation of molecules during heating is associated with the formation of a rotator R_{III} phase. Similarly to dotriacontane, there is every reason to believe that a high-temperature modification of M_{101} should also appear in triacontane in case of the transition from M_{011} to R_{III} . In turn, structural rearrangements should occur in dotriacontane and hexatriacontane through two rotator phases R_{III} and R_{IV} , as found in triacontane. At the same time, it is likely that the R_{IV} phase is a state which is very close to the melt, but in which the long-range order in the arrangement of molecules is still preserved.

Thermodynamic properties of some n -alkanes (with n from 16 to 25) were already studied in our previous papers [33–36] and dependences of thermodynamic parameters on the parity of the number of carbon atoms in the chain were found. The DSC method established that the transition from solid to liquid and back occurs in two stages in long n -alkanes (starting from $n = 20$ with even carbon numbers, starting from $n = 17$ with odd carbon numbers) in heating–cooling cycles. It was demonstrated

for the first time [37] that if DSC method-specific errors are eliminated it is possible to determine actual thermodynamic parameters of phase transitions, in particular, presence of a true temperature hysteresis. It was found based on the presence/absence of true hysteresis and analysis of the shape of the heat capacity peaks that the low-temperature solid-solid phase transition is a phase transition of the I first order (PT-1) due to a change of the type of symmetry of the packing of molecules in the crystal cores of nanolamels, and the high-temperature phase transition corresponds to a second order phase transition (PT-2) of order–disorder type accompanied by melting/crystallization of n-alkane. At the same time, it turned out that PT-1 develops in case of heating in a relatively wide temperature range of $\Delta T = 1\text{--}3^\circ\text{C}$, which made it possible to attribute such transitions to diffuse phase transitions (DPT) [38–40]. The developed theory of such transitions [33,37,40] considers the heterogeneous mechanism of the structural transition by the fluctuation occurrence of stable nanonuclei of a new phase (of a different symmetry relative to the initial one) in the crystal volume and the subsequent propagation of the resulting interphase boundary due to the step-by-step addition of nanonuclei to the region of the new phase.

In connection with the above, the purpose of this paper is to conduct precision studies of the phase transformation process in case of heating of n-alkanes with $n = 30, 32$ and 36 to establish the mechanism of structural transformations, which, as we assume, should be similar due to the identical crystal structure of homologues. Consideration of phase transformations from the point of view of the theory of diffuse phase transitions will allow for the first time to identify individual stages in the development of multistage phase transitions based on the analysis of the shape of peaks and to study them independently. This will make it possible to identify the features of the heterogeneous development of phase transitions, as well as to establish the generality or difference of their thermodynamic parameters. Thus, the data available in the literature on the mechanism of structural rearrangements in longer homologues of n-alkanes will be supplemented and to some extent the existing gaps in the series of their phase transformations will be closed.

2. Experiment

Commercial samples produced by Sigma-Aldrich with a purity of 98% for C30 and C36 and 97% for C32 were selected to study the features of phase transformations in the homological series of even n-alkanes: triacontane $\text{C}_{30}\text{H}_{62}$ (C30), dotriacontane $\text{C}_{32}\text{H}_{66}$ (C32) and hexatriacontane $\text{C}_{36}\text{H}_{74}$ (C36).

The thermophysical properties of n-alkanes were studied by differential scanning calorimetry using DSC-500 calorimeter („Spetspribor“, Russia) in a nitrogen atmosphere. The temperature scale was calibrated by the melting points of ice (273.1 K) and indium (429.7 K); the heat flow scale was calibrated using the heat capacity

of leucosapphire. The weight of the test samples was 0.5–1.0 mg to ensure minimum thermal resistance of the calorimetric cell and reduce the methodological error.

The samples for the study were prepared as follows: several flakes were collected from commercial flake powders and were placed in a calorimetric cuvette in one layer and covered with a lid without additional pressing to prevent any structural changes.

The selected scanning speed was 0.25 K/min which was optimal for samples of a given mass, on the one hand, to achieve the best resolution of heat capacity peaks, on the other hand, to ensure sufficient intensity of heat capacity peaks for registration.

3. Results and discussion

At the first stage of the study, thermograms were acquired for each sample exclusively in the areas of solid-solid phase transitions during heating (without melting) followed by cooling to room temperature (Figure 1). This approach makes it possible to determine in case of reheating whether the observed transitions are reversible.

The thermograms in Figure 1 show double peaks of solid-solid phase transitions in C32 and C36, separated by several tenths of a degree Celsius on the temperature scale, as well as an asymmetric peak in C30, which suggests the presence of at least two stages in the development of these transitions.

The weak endothermic effect at 62.1°C in C32 is probably attributable to the low-energy transition of the initial orthorhombic phase to the monoclinic [13]. The presence of an orthorhombic phase may be caused by a lower purity of the homologue compared to other samples and is associated with a greater defect due to the presence of a minimum number of nearby homologues of other n-alkanes. The occurrence of an orthorhombic phase instead

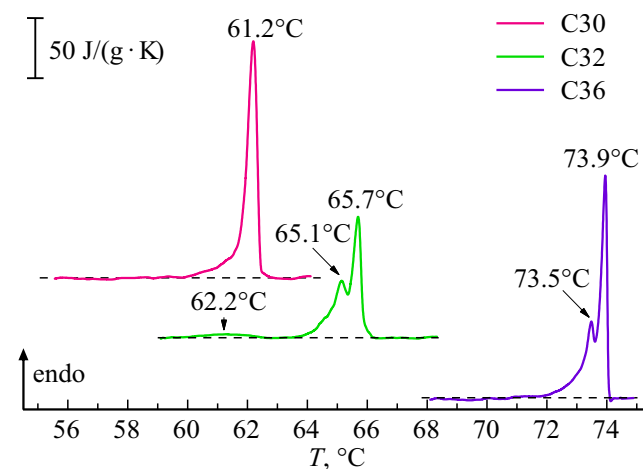


Figure 1. DSC thermograms of heating samples of triacontane (C30), dotriacontane (C32) and hexatriacontane (C36) in the region of solid-solid phase transitions.

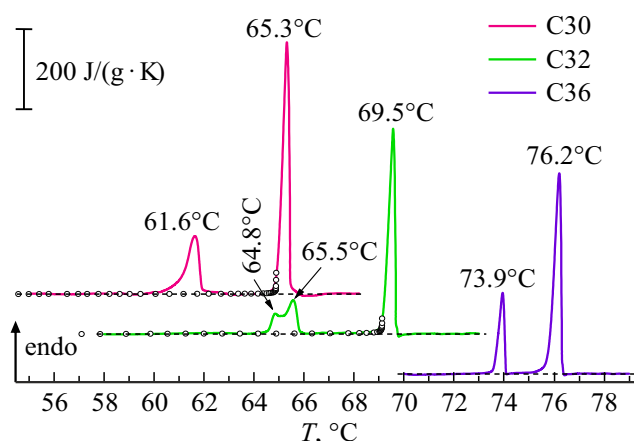


Figure 2. Thermograms of reheating samples of triacontane (C30), dotriacontane (C32) and hexatriacontane (C36) to the melt state. The circles represent the calculated dependencies by the ratio (1).

of an energetically stable monoclinic phase is typical for samples with purity < 98% [20,21,23].

A reheating of each sample with a „full cycle“ was carried out at the second stage of the study to establish the reversibility of solid-solid phase transitions: solid-solid phase transition + melting (Figure 2). As can be seen from the figure, the shape of the solid-solid phase transition peak has changed for C36: instead of two previously recorded maxima, only one is observed, while at the same time it corresponds in temperature to the high-temperature maximum on the previous curve (Figure 1). In addition, the enthalpy of the solid-solid phase transition decreased by 30% during reheating. A double peak of the solid-solid phase transition is still observed for C32, however, it is clear that the intensity of the second peak has slightly decreased, but at the same time the total half-width has increased. In general, the shape of the peak of the solid-solid phase transition does not change for C30, but there is also a slight decrease in intensity and an increase in the half-width of the peak. It is important to note that the enthalpy of the solid-solid phase transition is completely preserved for C30 and C32 in case of reheating.

From the comparison of Figure 1 and Figure 2, it can be concluded that the low-temperature transition in hexatriacontane (at 73.5°C) is an irreversible phase transition, probably related to the transition between two monoclinic modifications. There are no irreversible phase transitions in the triacontane and dotriacontane homologues. We attribute the observed small changes in the shape of peaks, especially in dotriacontane, to the presence of conformational defects in the initial samples due to their insufficient purity.

As can be seen from Figure 2, all curves demonstrate a low-temperature peak of the solid-solid phase transition with $T_{\max 1}$, as well as a high-temperature melting peak with $T_{\max 2}$. At the same time, there is a noticeable difference in both the enthalpy of transitions proportional to the peak

area and the temperatures $T_{\max 1}$ and $T_{\max 2}$. It should be noted that the shape of endothermic peaks has its own characteristics for each of the studied materials at a temperature $T_{\max 1}$. This picture generally corresponds to the results presented in previously published papers [4,8,32].

The DSC curves of reheating triacontane and dotriacontane samples were selected (Figure 2, C30 and C32) for a full-fledged analysis of the features of the peaks of solid-solid phase transitions, including the irreversible transition, since reheating allows to significantly eliminate conformational defects affecting the shape of PT-1. For hexatriacontane, this approach additionally eliminates an irreversible phase transition, therefore, in this case, the DSC heating curve of the initial sample was selected for analysis (Figure 1, C36), taking into account possible differences from other samples in the future.

It is necessary to eliminate the contribution to the heat capacity of the higher-temperature endothermic peak of the phase transition of the II order for a correct identification of the endothermic peak of the phase transition of the I order on the DSC curve. As it was shown in the papers of Landau [41] for phase transitions of the II order, the peak C_p has a λ -shape described at temperatures $T < T_{\max 2}$ by a power function of the type

$$C_p(T) = \alpha(T_{\max 2} - T)^{-0.5}, \quad (1)$$

where α — constant; $T_{\max 2}$ — the temperature of the phase transition of the II order.

Figure 2 shows calculated dependences C_p for the low-temperature part of the peak $T_{\max 2}$ based on the ratio (1) in light circles which best match the experimental data for the values of the parameters for triacontane $\alpha = 1.5$, $T_{\max 2} = 338.1$ K; for dotriacontane $\alpha = 2.2$, $T_{\max 2} = 342.3$ K. Since the calculated exponential function can be extended to the temperature range corresponding to the first order phase transition, this allows, after subtracting the calculated component from the experimental dependence C_p in the region $T_{\max 1}$ to clarify the shape of the peak corresponding to the phase transition of the I order. This approach cannot be applied for hexatriacontane due to the absence of a melting peak on the initial DSC curve, therefore, the baseline was subtracted, taking into account the obtained offsets for the other two samples.

Endothermic peaks corresponding to structural phase transitions of the I order were identified using the above approaches (Figure 3, black curves). Indeed, the shape of these peaks turned out to be clearly asymmetric, which suggests the presence of several components. These features of the peak shape will be discussed below.

The peaks obtained using the above method were analyzed according to the theory of diffuse phase transitions (DPT) [38,40] in relation to Λ -shaped solid-solid phase transitions of the first order. Paper [42] obtained the following relation for the temperature dependence of heat

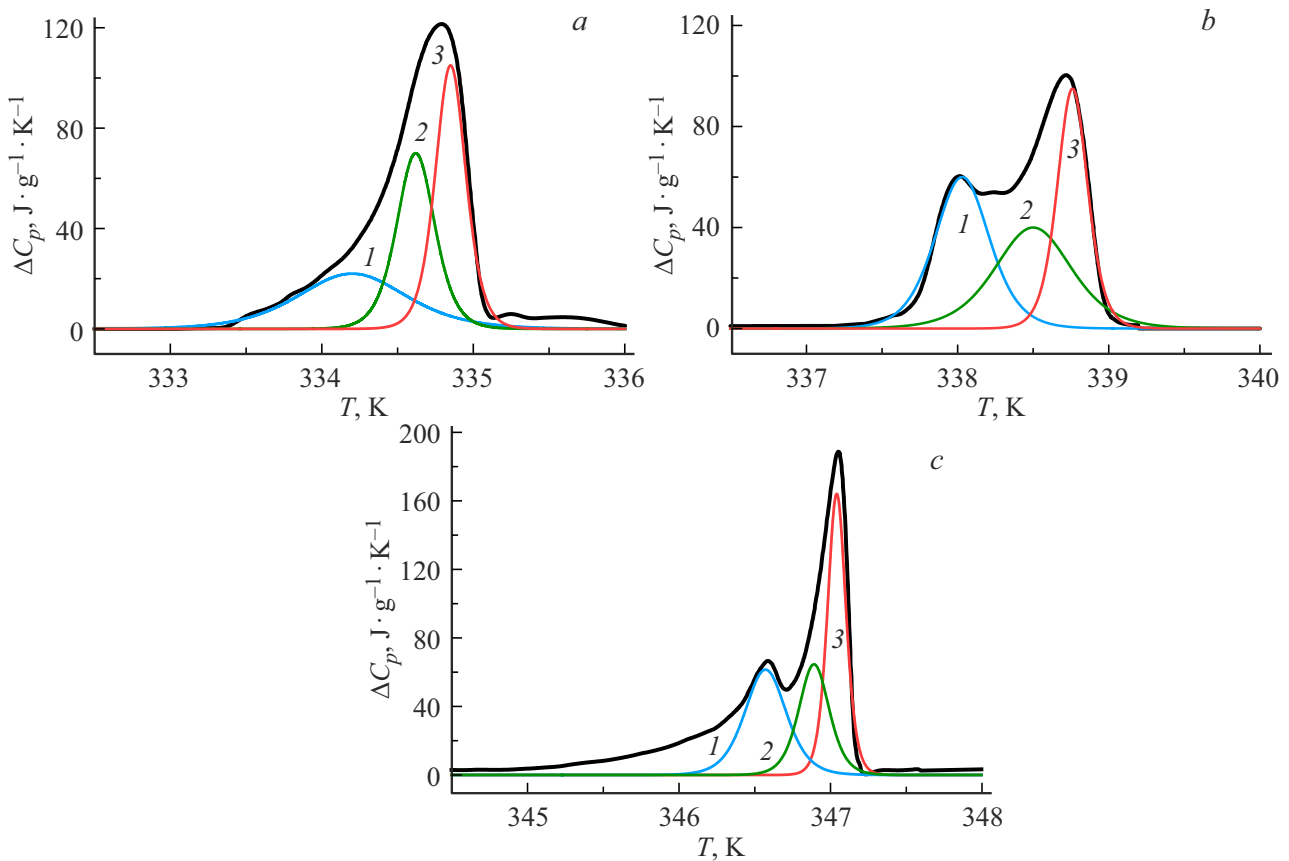


Figure 3. Decomposition of experimental heat capacity peaks (black curves) corresponding to solid-solid phase transitions in triacontane (a), dotriacontane (b) and hexatriacontane (c) into symmetric components (1, 2, 3).

capacity in case of the diffuse phase transition

$$\Delta C_p(T) = 4\Delta C_m \cdot \exp\left(B \frac{T - T_0}{T_0}\right) \times \left[1 + \exp\left(B \frac{T - T_0}{T_0}\right)\right]^{-2}, \quad (2)$$

where T_0 — the temperature of the phase transition of the first order; ΔC_m — the maximum value of the heat capacity at $T = T_0$; B — the athermal parameter.

Parameter B in the above ratio (2) contains the most interesting information about the physical nature of the phase transition, since it is related to the magnitude of the peak heat capacity ΔC_m :

$$\Delta C_m = \frac{q_0 B}{4T_0}, \quad (3)$$

where q_0 — the heat of transformation (enthalpy), and the elementary volume of transformation ω :

$$B = \frac{\omega \rho q_0}{k_0 T_0}, \quad (4)$$

where k_0 — Boltzmann constant, ρ — density. The parameter B is a structurally sensitive parameter, since it

determines the volume of nuclei of a new phase in materials with diffuse phase transitions. The values of the specific heat (enthalpy) of transformation q_0 can be found from ratio (3), the elementary volume of transformation ω can be found from the ratio (4).

It was noted above that the experimentally obtained peaks of phase transitions of the first order in the studied samples of n-alkanes have an asymmetric shape. However, according to the DPT theory, the heat capacity peaks of diffuse phase transitions of the I order should have a symmetrical Λ -shape described by the ratio (2). In this regard, the asymmetric peaks were divided into symmetrical components using the method developed by us, described in detail in Ref. [35]. One of the criteria for this separation is the condition that the enthalpy of the experimentally obtained asymmetric peak is equal to the sum of the enthalpy of the symmetrical peaks composing this peak. The results of this separation are shown in Figure 3 (curves 1, 2, 3), and the parameters calculated by the ratios (2,3,4) are listed in Table 1 (assuming that the density of crystals is $\rho(\text{C30}) = 0.810$; $\rho(\text{C32}) = 0.812$; $\rho(\text{C36}) = 0.814 \text{ g} \cdot \text{cm}^{-3}$ [43]). The decomposition of the protracted leading edge was not carried out for hexatriacontane, since it is probably associated with the formation of conformational defects, which was

Table 1. Thermodynamic parameters of phase transitions in the studied samples

Sample	№ peak	T_0	q_0	B	ΔC_m	ω	Phase transition
		K	J/g		J/gK	nm ³	
Triacontane C30	1	334.20	21.0	1400	22	380	$M_{011} \rightarrow O$
	2	334.62	23.4	4000	70	975	$O \rightarrow M_{101}$
	3	334.85	28.1	5000	105	1015	$M_{101} \rightarrow R_{III}$
Dotriacontane C32	1	338.03	29.0	2800	60	554	$M_{011} \rightarrow O$
	2	338.50	27.1	2000	40	425	$O \rightarrow M_{101}$
	3	338.77	25.4	5500	95	1247	$M_{101} \rightarrow R_{III}$
Hexatriacontane C36	1	346.57	22.5	3800	62	992	$M_{011} \rightarrow O$
	2	346.89	17.3	5200	65	1768	$O \rightarrow M_{101}$
	3	347.04	26.5	8600	164	1909	$M_{101} \rightarrow R_{III}$

observed for the rest of the samples on the initial DSC curves, unlike repeated curves.

Figure 3 shows that the peak of the solid-solid phase transition from the initial monoclinic structure to the rotator phase consists of several symmetrical Λ -shaped components in each of the studied samples. In this regard, we consider the development of a solid-solid phase transition as a multistage process associated with a discrete change of the crystallographic group of a monoclinic cell in this case, accompanied by a change of the inclination of molecules relative to the location of molecules in a finite rotatory structure. In addition, each of the stages is characterized by a certain type of nuclei of a new phase as can be seen from Table 1. Two types of nuclei can be distinguished, relatively small in the first stages and larger in the second and third stages of the phase transformation from M_{011} to R_{III} . The nuclei have nanometer sizes at all stages, but their size also increase with the increase of the length of the n-alkane chain.

Thus, it is possible to correlate the peaks of heat capacity with the ongoing phase transformations in all three samples (see Table 1). We attribute the peak of the heat capacity № 3, which has the highest intensity, to the transition to the rotator state of matter (in the phase R_{III}). A similar effect was observed in shorter n-alkanes [2–6]. As noted above, there should be a transition $M_{011} \rightarrow M_{101}$ before the transition to the rotator state, proceeding through the formation of an intermediate orthorhombic O phase. As a result, we associate the peak № 1 with the phase transition $M_{011} \rightarrow O$, and the peak № 2 — with the transition $O \rightarrow M_{101}$. The transition to phase R_{IV} in case of heating cannot be registered for any of the samples due to the low intensity of the corresponding peak of heat capacity against the background of the melting peak.

4. Characterization of the nuclei of new phases in the homological series of n-alkanes

As shown in our previous paper [36] the solid-solid phase transition is also a multistage process in a large group of n-alkanes with both an even number and an odd number of carbon atoms in the chain. The values ω obtained in this paper allow drawing up an overall picture of the change of phase volumes depending on the length of the chain n . Such dependences are shown in Figure 4 for n-alkanes with odd (Figure 4, *a*) and even n (Figure 4, *b*).

The results presented in Figure 4, *a* and Figure 4, *b* demonstrate significant differences in the behavior of dependencies $\omega(n)$ for even and odd n-alkanes.

If the elementary volumes of transformation ω are almost independent of the chain length at the first stage of solid-solid phase transitions for odd n-alkanes (Figure 4, *a*, curve 1), which is also observed for short even n-alkanes (Figure 4, *b*, curve 1), then an increase of the chain length of even n-alkanes is characterized by almost a twofold continuous increase of volumes ω with a relatively small increase of the number of carbon atoms in the chain (from 24 to 32) and the subsequent sharper increase of ω in the area of $n = 32–36$ to values around 1000 nm³.

A sharp increase of the volume of nanonuclei up to $\omega \approx 2000–3000$ nm³ is observed at the second stage of transitions for both even and odd n-alkanes. At the same time, the dependence $\omega(n)$ in the odd n-alkanes is characterized by the continuous growth (Figure 4, *b*, curve 2) reaching saturation at $\omega \approx 2700$ nm³ for relatively small lengths of molecules $n = 25$. At the same time, this dependence is complex for even n-alkanes, however it demonstrates an increase to $\omega \approx 2000$ nm³, which can be compared with the site for $n = 19–21$ in Figure 4, *a* assuming saturation at $n \sim 40–44$.

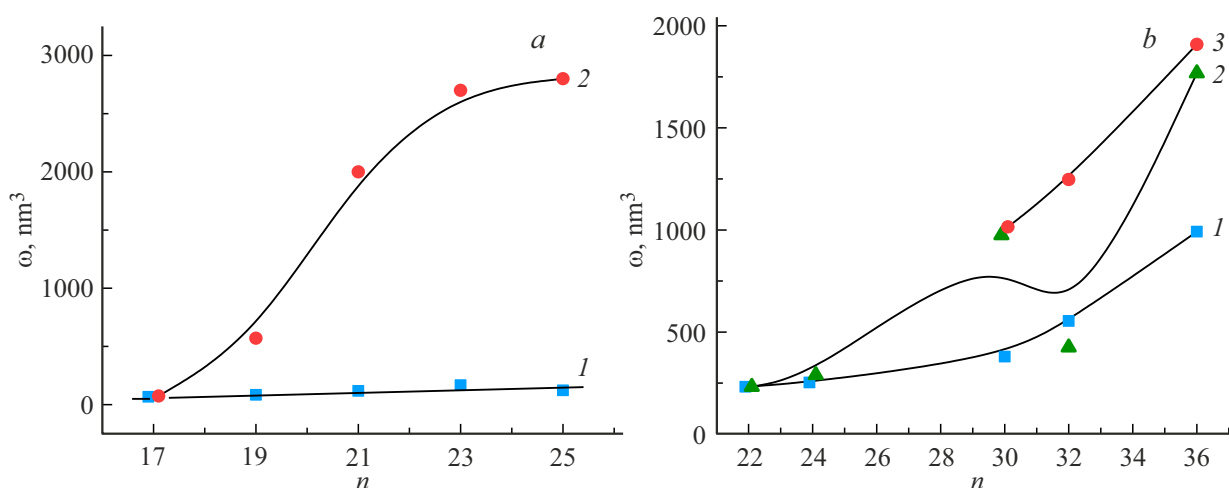


Figure 4. Elementary transformation volumes ω at the first (curves 1), second (curves 2) and third (curve 3) stages of the phase transition in n-alkanes with odd carbon numbers (a) and in n-alkanes with even carbon numbers (b) in the chain.

A very sharp dependence $\omega(n)$ in the region of n from 30 to 36 should be noted at the third stage of phase transitions, characteristic only for even n-alkanes of the longest chain lengths (considered in this paper). In general, the third stage in these samples can be correlated with the second in shorter samples, since the transition to the rotator phase occurs at that particular phase, as well as at the second stage of odd and short even n-alkanes.

The increase of the dependences $\omega(n)$ may be attributable to an increase of the thickness of the n-alkane lamellae (L_0) as the n grows. The value of L_0 can be determined for each of the phases by the expression $L_0 = c \cdot \sin\beta$, where c is the parameter of the main lattice cell (for the case of single-layer packing of molecules), and β is the angle of inclination of the molecules in the lamellae. The nuclei of the orthorhombic O phase are formed at the first stage of the transition for long n-alkanes such as triacontane, dotriacontane and hexatriacontane, the nuclei of the monoclinic M_{101} phase are formed at the second stage, and the nuclei of the rotator phase R_{III} are formed at the third. The parameters $c = L_0$ for phase O ($\beta = 90^\circ$) in C30, C32 and C36 were obtained in Ref. [44], and parameters $c = 4.827$ nm and $\beta = 106.0^\circ$ for M_{101} in C36 were defined in the article [31]. The parameters c and angles β for M_{101} in C30 and C32 are not available in the literature, however, it is possible to approximately calculate the values L_0 for C30 and C32 based on the data for C36. The exact parameters of both main cell and subcell have not yet been determined for the rotator phase R_{III} , as mentioned above. However, in this case it is possible to approximately calculate L_0 for R_{III} in C30, C32 and C36 based on the data of Ref. [13]. The results of calculation of L_0 for all phases are presented in Table 2.

In shorter n-alkanes with $n = 17$ – 25 , nuclei of the rotator phases R_I and R_{II} are formed at both stages of the solid-solid phase transition for odd and even n-alkanes, respectively [36]. Since both phases R_I and R_{II} have

Table 2. The thickness of the lamellae in each of the new phases in case of the solid-solid phase transition

Sample	$L_0(O)$ [44]	$L_0(M_{101})$	$L_0(R_{III})$
	nm	nm	nm
Triacontane C30	4.00	3.90	4.03
Dotriacontane C32	4.27	4.16	4.30
Hexatriacontane C36	4.76	4.64	4.84

a vertical arrangement of molecules relative to the base planes of the lamellae, the thickness of the lamellae L_0 for all short n-alkanes can be approximately calculated using the expression $L_0 = l_0 \cdot n$, where $l_0 = 0.1273$ nm is the magnitude of the projection of the bond C–C onto the axis of the molecule.

By estimating the thickness (L) of nanonuclei based on the dependence $L = 1.1 \cdot \omega^{1/3}$ [33], it is possible to determine in which number of n-alkane lamellae (k) the nanonuclei is located, since $k = L/L_0$. Figure 5 shows the results of such a calculation based on the data ω from Figure 4 and the calculated values L_0 .

It can be seen from Figure 5 that the increase of dependencies observed in Figure 4 $\omega(n)$ is attributable to an increase of the length of the n-alkane chain. Thus, it turns out that nanonucleus is formed in two adjacent lamellae at the first stage taking into account this dependence for both even and odd n-alkanes. At the same time, this process in both cases covers a larger number of lamellae in the second stage. At the same time, the second stage begins at small n (from $n = 17$) in the odd n-alkanes and in the extreme case covers an extended stack of 5 lamellae. Whereas this occurs at large n (from $n = 24$) in even n-alkanes, and the maximum elementary volume of phase transformation

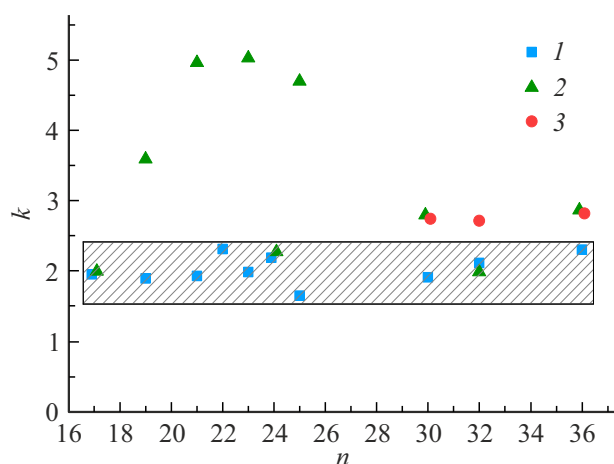


Figure 5. Dependence of the number of n-alkane lamellae on the number of carbon atoms in the chain involved in the formation of the elementary volume ω on the first (1), the second (2) and the third (3) the stages of phase transformation.

is formed only in three adjacent lamellae, like in the third stage for long even n-alkanes.

The calculated number of lamellae of one nucleus in C30, C32 and C36 at the initial stages of transition is two lamellae, then increases to three, which generally corresponds to the shorter n-alkanes that we studied earlier.

5. Threshold length of the n-alkane chain for realization of a solid-solid phase transition

As it was seen from Figure 4, as the chain length decreases, the volumes of nuclei of both even and odd n-alkanes also decrease. It can be assumed that there is some value n_0 at which the volume of the nucleus turns to zero, i.e. no new phase is formed. When studying the homological series of n-alkanes, it is of considerable interest to determine the threshold value n_0 for the occurrence of a solid-solid phase transition, i.e., starting from which chain lengths structural rearrangements in the solid phase become possible.

It turned out that the analysis of the energy components of the minimum Gibbs free energy (ΔG), determined by the ratio between the bulk and surface energies of the elementary phase volume, allows establishing the minimum chain length n_0 , at which the formation of nuclei of a new phase is possible.

The contribution of surface energy from the lateral faces of the crystal is usually neglected when considering ΔG in the lamellar structure of polymers, in particular, when deriving the well-known Thomson–Gibbs equation. This is attributable to the fact that the end surface energy (γ_1) in folded polymer lamellae significantly exceeds the surface energy of the side faces of the crystal (γ_2). The values of γ_1 and γ_2 do not differ so much in long-chain molecular

crystals, in particular, in n-alkanes, since they are proportional to the cohesion energy of (E_c) of groups $-\text{CH}_3$ ($E_c = 4.14$ kJ/mol) and groups $-\text{CH}_2-$ ($E_c = 3.60$ kJ/mol) forming, respectively, the end and side surfaces of the elementary volume [45]. Therefore, it is necessary to take into account the contribution of lateral surface energy to the Gibbs free energy in n-alkanes. In this case, let us consider the elementary volume of transformation ω with a square cross-section area a^2 and the thickness of the nanonucleus $L = l_0 \cdot n \cdot k$, where $l_0 = 0.1273$ nm is the magnitude of the projection of the bond C–C per axis of the molecule, n is the number of carbon atoms in the n-alkane chain, and k is the number of lamellae in the nanonucleus. Therefore, ΔG will be determined by the following relation

$$\Delta G = -a^2 l_0 n k \Delta q(n) + 2a^2 \gamma_1 + 4a l_0 n k \gamma_2, \quad (5)$$

where $\Delta q(n)$ is the enthalpy of melting, which depends on the length of the n-alkane chain n . This dependence was experimentally established and has the following form: $\Delta q(n) = 4.1 \cdot n - 11$ (kJ/mol) [4].

The expression for parameter a of the elementary volume of transformation ω can be obtained by differentiating equation (5) for this parameter and equating the resulting expression to zero

$$a = 2l_0 n k \gamma_2 (l_0 n k \Delta q(n) - 2\gamma_1)^{-1}. \quad (6)$$

Further, since the value a should be positive, that is, $a > 0$, we obtain the following inequality taking into account the above experimental dependence $\Delta q(n)$

$$l_0 n k \Delta q(n) - 2\gamma_2 > 0. \quad (7)$$

Finding the integer values n at which this inequality holds allows determining the threshold value n_0 , at which a solid-solid state phase transition, that is, the formation of a new phase nucleus, becomes possible in n-alkanes. It is necessary to estimate the value of the end surface energy γ_2 of the lamella to solve the quadratic equation on the left side of the inequality, the surface layer of which in n-alkanes consists of groups $-\text{CH}_3$. The value γ_2 is determined by the fraction of the cohesion energy of one group $-\text{CH}_3$ ($\sim 0.4E_c$ [33]) per the cross-sectional area of one n-alkane molecule (S). The latter for all crystal cores of lamellae of the lowest symmetry category (triclinic, monoclinic, orthorhombic) has the value of $S \sim 0.16$ nm². The ratio $0.4E_c/S$ gives the sought value $\gamma_2 \approx 17$ erg/cm².

It should be noted that the estimated value of the end surface energy of n-alkane lamellae is significantly inferior to the surface energy of folded polyethylene lamellae, which is 87 erg/cm² [46]. This is attributable to the fact that the folded surface of the latter consists of so-called regular folds consisting of several gosh isomers, which significantly increase the excess energy of the surface layer of the lamellae. At the same time, the lateral surface energy of the n-alkane lamellae should be equal to the lateral surface

energy of the folded polyethylene lamellae, since they have the same internal structure formed by the groups $-\text{CH}_2-$.

Solving the quadratic equation on the left side of the inequality (7) allows determining the threshold integer value $n_0 = 4$ at which this inequality holds.

Thus, the solid-solid phase transition should occur in all n-alkanes containing 4 or more carbon atoms in the chain. However, the solid-solid phase transition may not be experimentally detected, since the temperature of this transition may be in close proximity to the melting/crystallization temperature.

6. Conclusion

As a result of this study, it was possible for the first time to find a single sequence of multistage phase transformations in the solid state in the homological series of even n-alkanes: triacontane $\text{C}_{30}\text{H}_{62}$ dotriacontane $\text{C}_{32}\text{H}_{66}$ and hexatriacontane $\text{C}_{36}\text{H}_{74}$. The presence of three stages was revealed in the region of the commonly observed solid-solid phase transition: $M_{011} \rightarrow O$; $O \rightarrow M_{101}$; $M_{101} \rightarrow R_{\text{III}}$, each of which is an individual heterogeneous phase transition. The habitus (shape) of the nanonuclei of the new phase was determined for each of the stages which was lamellar in each case with a varying number of lamellae in the nanonuclei — from two to three, depending on the phase.

Thus, the transition from the monoclinic M_{011} to the rotator R_{III} phase should occur sequentially in the considered homologues of n-alkanes through two intermediate phases — orthorhombic O and monoclinic M_{101} . In addition, such a mechanism can be assumed to be uniform in all n-alkanes with initial M_{011} and rotator R_{III} phases.

The first phase transformation $M_{011} \rightarrow O$ corresponds to the transition from the initial monoclinic modification (the inclination of molecules in the bc -plane) to the main orthorhombic cell with a vertical arrangement of molecules, the nuclei of the new phase in this case cover two lamellae, which is typical for shorter n-alkanes. Then the second phase transformation $O \rightarrow M_{101}$ occurs, as a result of which the molecules are again stacked in the main cells with monoclinic symmetry, but with an inclination already in the ac -plane. The nuclei of the new phase slightly increase at the second stage $O \rightarrow M_{101}$ and their habitus includes two or three lamellae, depending on the sample. The third phase transformation is the transition $M_{101} \rightarrow R_{\text{III}}$, i.e. the transformation of the main cells of monoclinic symmetry into triclinic rotator cells with the possibility of discrete rotation of molecules around their axes in lamellae. This transition is accompanied by the formation of the largest nuclei comprising three lamellae in each case. In general, the heterogeneous nature of phase transformations in extended n-alkanes with $n = 32-36$ corresponds to two stages of solid-solid phase transition in shorter n-alkanes, with the formation of smaller nuclei at the first stage and larger ones at the subsequent one.

The analysis of the data obtained made it possible to calculate the threshold chain length, starting from which solid-solid phase transitions become possible in lamellar crystals of n-alkanes. It turned out that the solid-solid phase transition, accompanied by a change in the type of symmetry of crystals, can occur in n-alkanes containing 4 or more carbon atoms in the chain.

Conflict of interest

The authors declare that they have no conflict of interest.

References

- [1] M.G. Broadhurst. *J. Res. Natl. Bur. Stand.* **66A**, 3, 241 (1962).
- [2] E.B. Sirota, H.E. King, D.M. Singer, H.H. Shao. *J. Chem. Phys.* **98**, 7, 5809 (1993).
- [3] E.B. Sirota, D.M. Singer. *J. Chem. Phys.* **101**, 12, 10873 (1994).
- [4] A.-J. Briard, M. Bouroukba, D. Petitjean, N. Hubert, M. Dirand. *J. Chem. Eng. Data.* **48**, 3, 497 (2003).
- [5] S. Nene, E. Karhu, R.L. Flemming, J.L. Hutter. *J. Cryst. Growth.* **311**, 4770 (2009).
- [6] E. Blázquez-Blázquez, R. Barranco-García, M.L. Cerrada, J.C. Martínez, E. Pérez. *Polymers* **12**, 6, 1341 (2020).
- [7] D. Cholakova, K. Tsvetkova, S. Tcholakova, N. Denkov. *Colloids Surf. A: Physicochem. Eng. Asp.* **634**, 127926 (2022).
- [8] C.M. Earnest, J. Jones, A. Dunn. *Thermo* **2**, 302 (2022).
- [9] J. Doucet, I. Denicolò, A.F. Craievich. *J. Chem. Phys.* **75**, 3, 1523 (1981).
- [10] J. Doucet, I. Denicolò, A.F. Craievich, A. Collet. *J. Chem. Phys.* **75**, 10, 5125 (1981).
- [11] I. Denicolò, J. Doucet, A.F. Craievich. *J. Chem. Phys.* **78**, 3, 1465 (1983).
- [12] G. Ungar. *J. Phys. Chem.* **87**, 4, 689 (1983).
- [13] J. Doucet, I. Denicolò, A.F. Craievich, C. Germain. *J. Chem. Phys.* **80**, 4, 1647 (1984).
- [14] M. Dirand, M. Bouroukba, V. Chevallier, D. Petitjean, E. Behar, V. Ruffier-Meray. *J. Chem. Eng. Data* **47**, 2, 115 (2002).
- [15] A. Müller. *Proc. Royal Soc.* **A138**, 836, 514 (1932).
- [16] A.I. Kitaigorodsky. *Molekulyarnyye kristally.* Nauka, M. (1971). 424 s. (in Russian).
- [17] B. Ewen, D. Richter. *J. Chem. Phys.* **69**, 7, 2954 (1978).
- [18] J.-P. Gorce, S.J. Spells, X.-B. Zeng, G. Ungar. *J. Phys. Chem. B* **108**, 10, 3130 (2004).
- [19] P.A.S.R. Wickramarachchi, S.J. Spells, D.S.M. de Silva. *J. Phys. Chem. B* **111**, 7, 1604 (2007).
- [20] H.M.M. Shearer, V. Vand. *Acta Cryst.* **9**, 379 (1956).
- [21] P.W. Teare. *Acta Cryst.* **12**, 294 (1959).
- [22] A. Keller. *Philos. Mag.* **6**, 329 (1961).
- [23] A.A. Schaefer, C.J. Busso, A.E. Smith, L.B. Skinner. *J. Am. Chem. Soc.* **77**, 2017 (1955).
- [24] P.R. Templin. *Ind. Eng. Chem.* **48**, 154 (1956).
- [25] P.K. Sullivan. *J. Res. Natl. Bur. Stand.* **78A**, 2, 129 (1974).
- [26] K. Takamizawa, Y. Ogawa, T. Oyama. *Polym. J.* **14**, 6, 441 (1982).
- [27] C.M.L. Atkinson, M.J. Richardson. *Trans. Faraday Soc.* **65**, 1749 (1969).

- [28] P.K. Sullivan, J.J. Weeks. *J. Res. Natl. Bur. Stand.* **74A**, 2, 203 (1970).
- [29] T. Asano. *J. Phys. Soc. Jpn.* **54**, 4, 1403 (1985).
- [30] T. Asano, Md.F. Mina, I. Hatta. *J. Phys. Soc. Jpn.* **65**, 6, 1699 (1996).
- [31] Md.F. Mina, T. Asano, H. Takahashi, I. Natta, K. Ito, Y. Ame-miya. *Jpn. J. Appl. Phys.* **36**, 5616 (1997).
- [32] K.-i. Tozaki, H. Inaba, H. Hayashi, C. Quan, N. Nemoto, T. Kimura. *Thermochimica Acta* **397**, 155 (2003).
- [33] V.M. Egorov, V.A. Marikhin. *Phys. Solid State* **58**, 12, 2574 (2016).
- [34] V.M. Egorov, V.A. Marikhin, L.P. Myasnikova, P.N. Yakushev. *Phys. Solid State* **59**, 10, 2070 (2017).
- [35] V.M. Egorov, A.K. Borisov, V.A. Marikhin. *Phys. Solid State* **63**, 3, 498 (2021).
- [36] A.K. Borisov, V.A. Marikhin, V.M. Egorov. *Phys. Solid State* **66**, 5, 726 (2024).
- [37] V.M. Egorov, V.A. Marikhin, L.P. Myasnikova. *Vysokomolek. soed.* **47B**, 339 (2005).
- [38] M.E. Fisher. *The nature of critical points*. University of Colorado Press, Boulder, Colorado, U.S.A. (1965). 159 p.
- [39] B.N. Rolov, V.E. Yurkevitch. *Fizika razmytykh fazovykh perekhodov*. Izd-vo Rostov. un-ta, Rostov (1983). 350 s. (in Russian).
- [40] G.A. Malygin. *UFN*, **44**, 173 (2001).
- [41] L.D. Landau, E.M. Lifshitz. *Statistical Physics*. Addison-Wesley. (1986). 484 p.
- [42] G.A. Malygin. *Phys. Solid State* **43**, 1909 (2001).
- [43] W.M. Haynes. *CRC Handbook of Chemistry and Physics* (96th ed.). CRC Press/Taylor and Francis, Boca Raton, FL. (2015). 2677 p.
- [44] S.C. Nyburg, J.A. Potworowski. *Acta Cryst. B* **29**, 347 (1973).
- [45] D.W. Van Krevelen. *Properties of polymers correlations with chemical structure*. N.Y. (1972). 480 p.
- [46] B.Wunderlich. *Macromolecular physics*. V. 1. Academic Press, New York, U.S.A. (1976). 472 p.

Translated by A.Akhtyamov